Spectral properties of the Peregrine soliton observed in a water wave tank

A. Chabchoub,[1] S. Neumann,[1] N. P. Hoffmann,[1] and N. Akhmediev[2]

Received 6 October 2011; revised 1 December 2011; accepted 2 December 2011; published 7 February 2012.

[1] The Peregrine soliton, which is commonly considered to be a prototype of a rogue wave in deep water, is observed and measured in a wave tank. Using the measured data of water elevation, we calculated the spectra of the Peregrine soliton and confirmed that they have triangular shapes, in accordance with the theory.

Citation: Chabchoub, A., S. Neumann, N. P. Hoffmann, and N. Akhmediev (2012), Spectral properties of the Peregrine soliton observed in a water wave tank, *J. Geophys. Res.*, *117*, C00J03, doi:10.1029/2011JC007671.

[2] Today, the existence of oceanic rogue waves is no longer doubted or considered to be a myth. Buoy, platform and satellite measurements as well as possible occurrence mechanisms are widely discussed in the literature [*Kharif et al.*, 2009; *Garret and Gemmrich*, 2009; *Osborne*, 2010; *Müller et al.*, 2005; *Onorato et al.*, 2001; *Ten and Tomita*, 2006]. (see also the proceedings of the MaxWave Final Meeting, World Meteorological Organization, Geneva, Switzerland, 8–10 October 2003). The direct measurements of the wave profiles or their reconstruction from the space photos are essential modern experimental techniques. They allow us to see the presence of rogue waves in a chaotic wavefield. Due to the nature of rogue waves that "appear from nowhere," more sophisticated techniques are needed if we want to predict the potential growth of rogue waves at earlier stages of their evolution. In optics, the spectral data are one of the main sets of measurements in experiments that allow us to reveal the presence of rogue waves in fibers [*Hammani et al.*, 2011a, 2011b]. The spectral approach in the case of ocean waves is also highly informative. The Hilbert spectrum analysis has been suggested as one of the ways to study the nonlinear evolution processes of Stokes waves [*Huang et al.*, 1999]. It was shown that this method provides a more precise definition of particular events in time-frequency space than wavelet analysis. It also provides more physically meaningful interpretations of the underlying dynamic processes. The direct spectral measurements for ocean waves have also been proposed as one of these promising methods [*Akhmediev et al.*, 2011a]. When these measurements are done progressively on patch by patch basis, the results may provide valuable information about raising amplitudes of rogue waves in certain region of the sea [*Akhmediev et al.*, 2011b]. Although, basic techniques have been described earlier, presenting them to the oceanographic community is one of the important aspects of research activity. We base our present spectral analysis on the water tank experiment published earlier [*Chabchoub et al.*, 2011].

[3] The Peregrine soliton is presently considered to be one of the possible candidates for description of rogue waves in deep waters [*Shrira and Geogjaev*, 2010]. It is the lowest-order rational solution of the nonlinear Schrödinger equation (NLS) and in contrast to other types of localized solutions it grows according to a power law rather than exponentially. This means that it takes significantly longer time for its amplification than for other breathers [*Dysthe and Trulsen*, 1999]. If this growth could be anticipated at early stages of the rogue wave formation, we may have more time to react. The main idea is that spectral measurements may separate the rogue wave component from others in the chaotic wavefield [*Akhmediev et al.*, 2011b] thus making the process of its growth to be visible in advance.

[4] In this work, we measure the spectral content of the Peregrine soliton that we observed in a water wave tank earlier [*Chabchoub et al.*, 2011]. We perform such measurements processing the amplitude data and transforming them into spectra. This technique provides us with the proof of principle. This way, we confirmed that the spectra of the Peregrine soliton have specific triangular shape as predicted theoretically. In order to see the spectra directly, special spectral equipment must be developed which presently does not exist. However, our technique may become promising and such equipment could be developed later and used for early warning in the oceanic conditions.

[5] Mathematical models which describe the formation of the extreme waves due to modulation instability [*Benjamin and Feir*, 1967] are based on nonlinear equations. The simplest one is the nonlinear Schrödinger equation (NLS) first derived by *Zakharov* [1968]:

$$i\left(\frac{\partial a}{\partial t}+c_g\frac{\partial a}{\partial x}\right)-\frac{\omega_0}{8k_0^2}\frac{\partial^2 a}{\partial x^2}-\frac{\omega_0 k_0^2}{2}|a|^2 a=0, \qquad (1)$$

where k_0 and $\omega_0 = \omega(k_0)$ denote the wave number and the frequency of the carrier wave, respectively. ω_0 and k_0 are connected through the dispersion relation of linear deep water wave theory $\omega_0 = \sqrt{gk_0}$, where g denotes the

[1]Mechanics and Ocean Engineering, Hamburg University of Technology, Hamburg, Germany.
[2]Optical Sciences Group, Research School of Physics and Engineering, Australian National University, Canberra, ACT, Australia.

0148-0227/12/2011JC007671

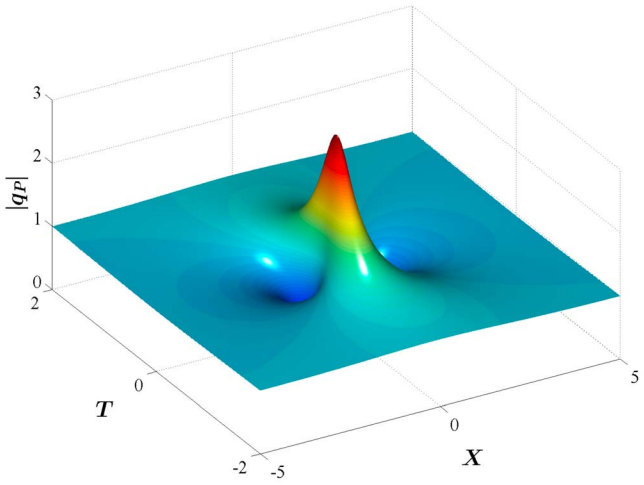

Figure 1. Peregrine breather solution $q_P(X, T) = \exp(2iT) \cdot (1 - \frac{4(1+4iT)}{1+4X^2+16T^2})$ of the focusing and rescaled (dimensionless) NLS: $iq_T + q_{XX} + 2|q|^2 q = 0$. Modified from *Chabchoub et al.* [2011], copyright 2011 by the American Physical Society.

gravitational acceleration. Envelope soliton solutions of the NLS interact with the background wave and propagate with the group velocity $c_g := \frac{\omega_0}{2k_0}$. The surface elevation $\eta(x, t)$ of the sea surface is then given by:

$$\eta(x,t) = \mathrm{Re}(a(x,t) \cdot \exp[i(k_0 x - \omega_0 t + \phi)]). \quad (2)$$

where ϕ is the carrier envelope phase.

[6] One of the prototypes of oceanic rogue waves described by the NLS (1) is the Peregrine solution [*Shrira and Geogjaev*, 2010; *Peregrine*, 1983]:

$$q_P(x,t) = a_0 \exp\left(-\frac{ik_0^2 a_0^2 \omega_0}{2} t\right) \times \left(1? \frac{4\left(1?ik_0^2 a_0^2 \omega_0 t\right)}{1 + \left[2\sqrt{2}k_0^2 a_0 (x - c_g t)\right]^2 + k_0^4 a_0^4 \omega_0^2 t^2}\right), \quad (3)$$

where a_0 is the amplitude of the carrier wave. Its special feature is that it is localized both in space and in time, thus being dubbed as a "wave that appears from nowhere and disappears without a trace" [*Akhmediev et al.*, 2009].This feature of the solution is clearly seen in Figure 1. It is worthy to mention that the Peregrine soliton is the limiting case of the space periodic Akhmediev breather [*Shrira and Geogjaev*, 2010; *Dysthe and Trulsen*, 1999; *Akhmediev and Korneev*, 1986; *Akhmediev et al.*, 1987] assuming the period to be infinite. In this limit, the amplitude of the breather occurred to be the highest while its amplification length being the longest. The latter fact is essential if we hope to base our early warning systems on these early stages of the rogue wave development.

[7] Despite the Peregrine soliton being one of the candidates [*Shrira and Geogjaev*, 2010] for description of rogue waves in the ocean the question will always remain to what extent this simplest solution of the NLS is close to the measured extreme waves. In this regard, we used the data of the Yura wave recorded in the Sea of Japan [*Liu and Mori*, 2001] and compared these data with the wave envelope given by the suitably normalized Peregrine soliton.

[8] Using the measured time series, we determined the characteristic frequency and amplitude of the Yura wave and used them for normalization of the theoretical curve. The comparison is shown in Figure 2. Although other explanations can be suggested, for chaotic ocean waves, the similarity is clearly visible. We do realize that a single plot cannot prove the case. However, this similarity justifies our efforts in studying the Peregrine soliton in the laboratory. Spectra of this solution is our next important step in such exploration.

[9] The first experimental observation of the Peregrine soliton in a water wave tank was recently documented by *Chabchoub et al.* [2011] while in optics it has been observed by *Kibler et al.* [2010]. In optics, the spectra can be measured directly. Such measurements have shown that they do have triangular shape in accordance with the theory. However, for water waves, the measurements are not trivial and require special efforts. In the present work, we use the measurements of water elevation and transform them into the spectral data.

[10] The experiments are performed in a 15 m × 1.6 m × 1.5 m water wave tank with 1 m water depth which is described by *Chabchoub et al.* [2011]. A single-flap paddle activated by a hydraulic cylinder is located at one end of the tank. A wave absorbing beach at the opposite end of the tank is installed to inhibit wave reflections. We excited the carrier wave with the angular frequency ω_0 and the amplitude a_0 that were chosen to best fit the size of the tank and selected to be $\omega_0 = 2\pi f_0$, where $f_0 = 1.7$ Hz, and $a_0 = 0.01$ m, respectively. The surface elevation at many points along the tank was measured by a capacitance gauges with a sampling frequency of $f_s = 0.5$ kHz.

[11] In order to obtain the spectra of the experimentally measured Peregrine breathers, we can proceed in various ways. One of them is to calculate the spectra of the water elevation that includes the carrier wave. Such spectra usually consist of the triangular spectra of the Peregrine soliton plus the central peak attributed to the harmonic background wave which ideally would be a delta function [*Akhmediev et al.*, 2011a].

[12] Another way is to first identify the envelope of each measurement. This way, we can avoid the presence of the delta function and obtain purely the triangular spectra. When chosen this technique, the complex envelope of each signal can be computed by the use of the Hilbert transform **H** [see *Osborne*, 2010]. Figure 3 shows the results of measurements which capture the carrier wave as well as the envelope evolution along the water tank. Hilbert transform allows us to eliminate the fast oscillations of the carrier wave and deal with the complex envelope [*Huang et al.*, 1999; *Thrane et al.*, 2011]. As we found previously [*Chabchoub et al.*, 2011], the latter represents the Peregrine soliton evolution along the x axis.

[13] Each time series provides the complex envelope approximated by the Hilbert transform applied on each signal. We rearranged the discrete signals from $x^* = 0.10$ m to the maximum amplitude amplification position at $x^* = 9.10$ m by ignoring the group velocity, that is, by aligning the envelope modulations in time. Due to the

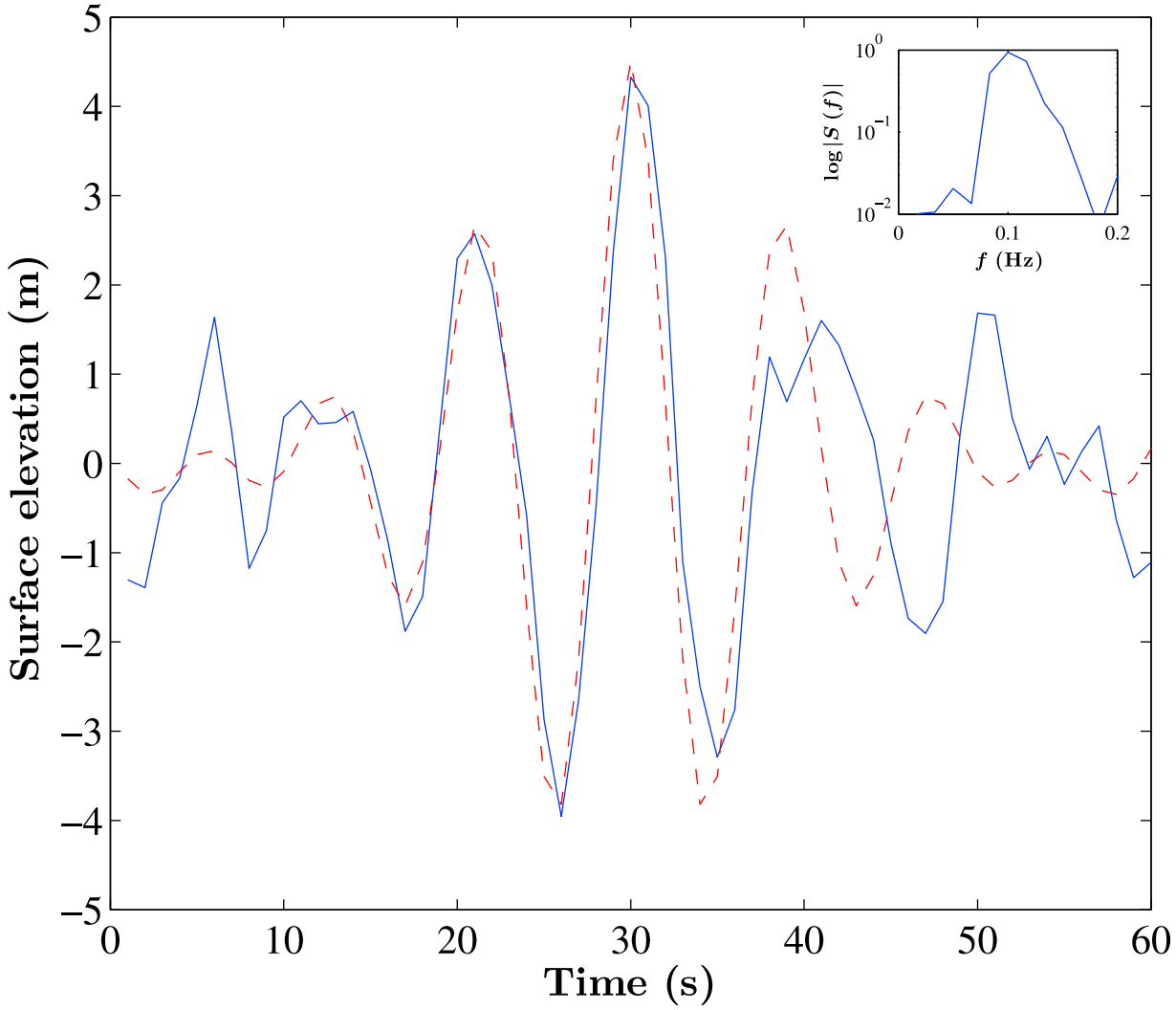

Figure 2. Yura wave data (solid blue curve) [*Liu and Mori*, 2001] compared with the normalized Peregrine breather solution combined with the carrier wave (dashed red line). The inset shows the spectrum of the Yura wave in the logarithmic scale calculated using the data of the present window.

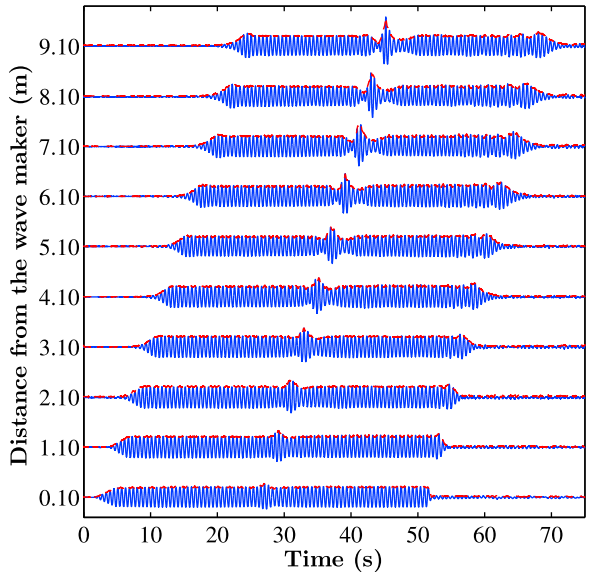

Figure 3. Evolution of the carrier in a water wave tank modeled by the Peregrine soliton (solid blue lines) and the envelope approximated by the modulus of the Hilbert transform $|\mathbf{H}[\eta(x^*, t)]|$ at a set of discrete positions along x axis (dashed red lines). Modified from *Chabchoub et al.* [2011], copyright 2011 by the American Physical Society.

symmetry of the Peregrine solution, the envelopes are then mirrored to catch the growth and decay process, as shown in Figure 4. This way, the length of evolution is doubled to 18 m. The plot has noise content as a result of the noise in the elevation data and the finite length of the carrier wave. Otherwise, the main features of the reconstructed Peregrine soliton are well presented. Having the envelope, we can calculate its spectrum.

[14] We use the discrete Fourier transform to calculate the spectrum of the Hilbert envelope over the 20 equidistant signals from position $x^* = -9.10$ m to $x^* = 9.10$ m as follows:

$$F(k, x^*) = \sum_{n=1}^{N} |\mathbf{H}[\eta(x^*, t)]| e^{\frac{-2\pi i(n-1)(k-1)}{N}}, \quad (4)$$

where N labels the length of the time series $\eta(x^*, t)$. Then, in order to obtain the correct frequency scale, $F(k, x^*)$ is mapped onto a frequency vector $f(k, x^*) = \frac{f_s k}{N}$. Finally, the frequency spectrum is estimated by:

$$S(f, x^*) = 2|F(f, x^*)|^2. \quad (5)$$

[15] Figure 5 shows the frequency spectrum of the reconstructed Peregrine soliton on a log scale evaluated at the 20 discrete space positions. Figure 5 clearly shows that the shape of the central part of the spectrum is triangular at any x. This feature was also experimentally observed in fibre optics [*Kibler et al.*, 2010]. Our water wave experiments confirm qualitatively the analytical results described by *Akhmediev et al.* [2011a]. These results demonstrate clearly the possibility of a rogue wave early warning through spectral measurements.

[16] In another set of calculations, we obtained the shape of the spectra directly from the measurements. Again, we used the discrete Fourier transform to calculate the spectra over the 20 equidistant signals, that is, from the point at the position $x^* = -9.10$ m to the point $x^* = 9.10$ m by computing the discrete Fourier transform:

$$F(k, x^*) = \sum_{n=1}^{N} \eta(x^*, t) e^{\frac{-2\pi i(n-1)(k-1)}{N}}, \quad (6)$$

Next, the function $F(k, x^*)$ is mapped onto a frequency vector $f(k, x^*) = \frac{f_s k}{N}$. Last, the frequency spectrum is estimated by:

$$S(f, x^*) = 2|F(f, x^*)|^2. \quad (7)$$

The results of these calculations are presented in Figure 6. We can see, from Figure 6, that for each x, the peak of the spectrum on a log scale is exactly located at 1.7 Hz which is the frequency of the background wave. The noise is also significantly lower. The latter is attributed to the direct way of calculations.

[17] For the sake of comparison, we also calculated the spectrum of Yura wave. It is presented in the inset of Figure 2. The spectrum is shown in the logarithmic scale and calculated in the same window as in Figure 2. Unfortunately, the number of data points in the experimental series is insufficient to make definitive conclusion. Nevertheless, the triangular shape of the spectrum can be seen even in this plot with limited number of data points.

[18] Spectra of water waves often involve components that correspond to bounded waves [*Huang et al.*, 1999; *Plant et al.*, 2004]. In our case, the second harmonic of the carrier frequency is located at 3.4 Hz = 2 × 1.7 Hz. The small peak at this frequency does exist but can be ignored for the wave amplitudes and wavelengths we are dealing with. The

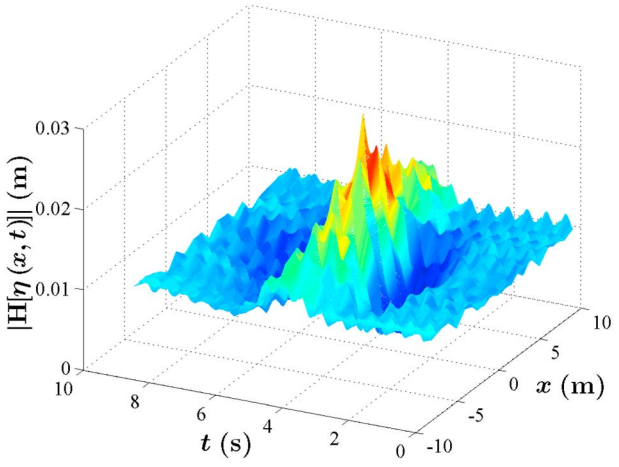

Figure 4. Reconstructed Peregrine breather from the Hilbert transform applied on each time series. The ripples are caused by the unavoidable noise in the experimental time series.

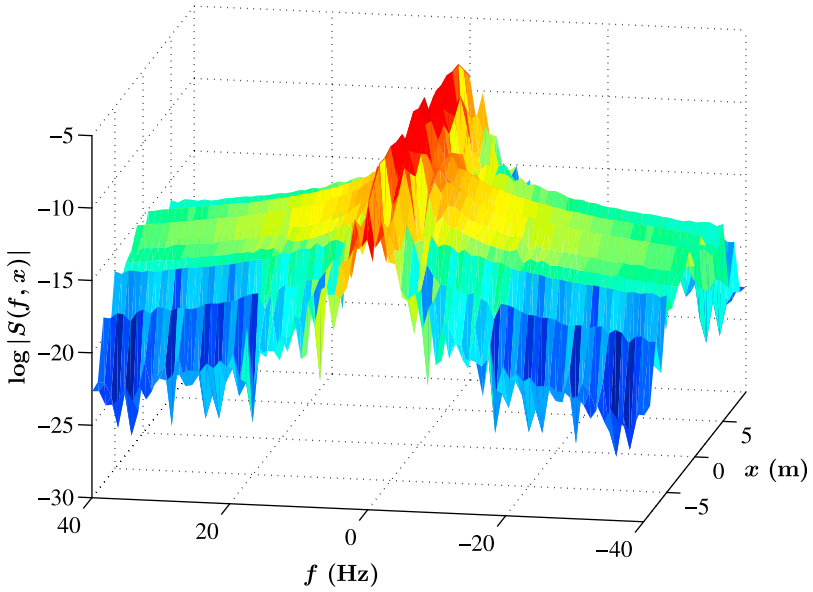

Figure 5. Spectrum on a log scale of the reconstructed Peregrine breather.

peak at the second harmonics becomes noticeable in case of wave amplitudes and wavelengths larger than 0.01 m and 0.54 m, respectively. However, our tank size cannot allow this as the deep water conditions then would not be satisfied.

[19] Finally, we should comment that in the geophysical applications, the nonlinear Schrödinger equation and the Peregrine breather, in particular, are valid for weakly nonlinear waves. Improved envelope models (*Dysthe*'s [1979] equation and other extensions [*Sedletskii*, 2003; *Slunyaev*, 2005]) and strongly nonlinear Euler equations are presently also employed to predict characteristics of oceanic rogue waves and their statistics. The higher-order corrections may add to the modifications of spectra. Nevertheless, the lowest-order approach that we confirmed to be the case in our experiment is important and has to be studied in the first place before considering complicated modifications. Clearly, such modifications would not be possible without having the basic effect in place.

[20] In conclusion, we observed the Peregrine soliton in a water wave tank and using the surface elevation data calculated the spectra. The calculations revealed the spectra of triangular shape that are in qualitative agreement with theoretical predictions. We expect that direct spectral measurements may reveal the Peregrine soliton on a water

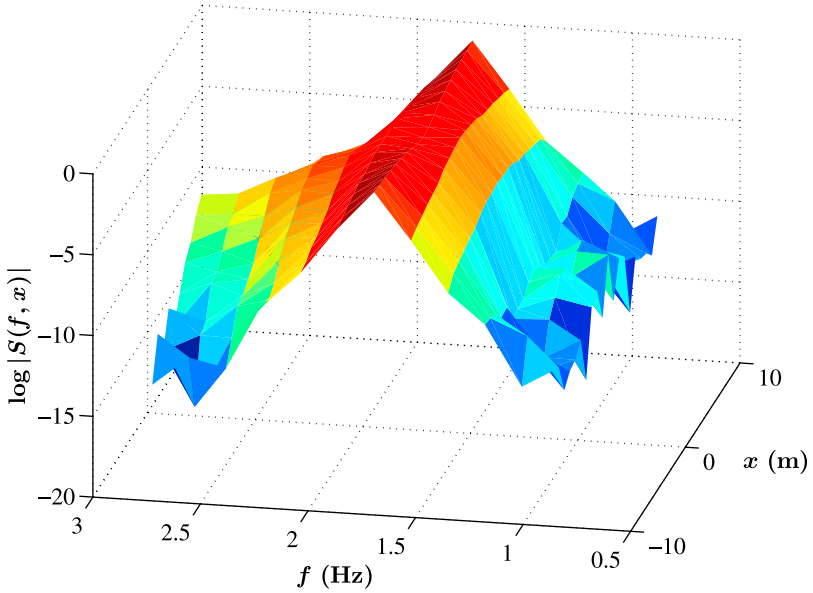

Figure 6. Spectrum on a log scale computed directly from the measurements.

surface before the main peak appears thus making an early warning possible from an experimental point of view.

[21] **Acknowledgments.** A. C., N. P. H and N. A. acknowledge Nobuhito Mori from Kyoto University for supplying us with the Yura data. N. A. and N. P. H. acknowledge the support of the Volkswagen Stiftung. N. A. acknowledges partial support of the Australian Research Council (Discovery Project DP110102068). N. A. is a recipient of the Alexander von Humboldt Award.

References

Akhmediev, N., and V. I. Korneev (1986), Modulation instability and periodic solutions of the nonlinear Schodinger equation, *Theor. Math. Phys.*, *69*, 1089–1093.

Akhmediev, N., V. M. Eleonskii, and N. Kulagin (1987), Exact first-order solutions of the nonlinear Schrödinger equation, *Theor. Math. Phys.*, *72*, 809–818.

Akhmediev, N., A. Ankiewicz, and M. Taki (2009), Waves that appear from nowhere and disappear without a trace, *Phys. Lett. A*, *373*, 675–678.

Akhmediev, N., A. Ankiewicz, J. M. Soto-Crespo, and J. M. Dudley (2011a), Rogue wave early warning through spectral measurements?, *Phys. Lett. A*, *375*, 541–544.

Akhmediev, N., J. M. Soto-Crespo, A. Ankiewicz, and N. Devine (2011b), Early detection of rogue waves in a chaotic wave field, *Phys. Lett. A*, *375*, 2999–3001.

Benjamin, T. B., and J. E. Feir (1967), The disintegration of wave trains on deep water. Part 1: Theory, *J. Fluid Mech. 27*, 417–430.

Chabchoub, A., N. P. Hoffmann, and N. Akhmediev (2011), Rogue wave observation in a water wave tank, *Phys. Rev. Lett.*, *106*, 204502.

Dysthe, K. B. (1979), Note on a modification to the nonlinear Schrödinger equation for application to deep water waves, *Proc. R. Soc. London, Ser. A*, *369*, 105–114.

Dysthe, K. B., and K. Trulsen (1999), Note on breather type solutions of the NLS as models for freak-waves, *Phys. Scr.*, *T82*, 48–52.

Garrett, C., and J. Gemmrich (2009), Rogue waves, *Phys. Today*, *62*, 57–59.

Hammani, K., B. Kibler, C. Finot, P. Morin, J. Fatome, J. M. Dudley, and G. Millot (2011a), Peregrine soliton generation and breakup in standard telecommunications fiber, *Opt. Lett.*, *36*, 112–114.

Hammani, K., B. Wetzel, B. Kibler, J. Fatome, C. Finot, G. Millot, N. Akhmediev, and J. M. Dudley (2011b), The spectral dynamics of modulation instability described using Akhmediev breather theory, *Opt. Lett.*, *36*, 2140–2142.

Huang, N. E., Z. Shen, and S. R. Long (1999), A new view of nonlinear water waves: The Hilbert spectrum, *Annu. Rev. Fluid Mech.*, *31*, 417–457.

Kharif, C., E. Pelinovsky, and A. Slunyaev (2009), *Rogue Waves in the Ocean*, Springer, Berlin.

Kibler, B., J. Fatome, C. Finot, G. Millot, F. Dias, G. Genty, N. Akhmediev, and J. M. Dudley (2010), The Peregrine soliton in nonlinear fibre optics, *Nat. Phys.*, *6*, 790–795.

Liu, P. C., and N. Mori (2001), Characterizing freak waves with wavelet transform analysis, in *Rogue Waves 2000*, pp. 151–156, Ifremer, Brest, France.

Müller, P., C. Garrett, and A. Osborne (2005), Rogue waves, the fourteenth 'Aha Huliko'a Hawaiian Winter Workshop, *Oceanography*, *18*, 185–193.

Onorato, M., A. Osborne, M. Serio, and S. Bertone (2001), Freak waves in random oceanic sea states, *Phys. Rev. Lett.*, *86*, 5831–5834.

Osborne, A. (2010), *Nonlinear Ocean Waves and the Inverse Scattering Transform*, Academic, Burlington, Mass.

Peregrine, D. H. (1983), Water waves, nonlinear Schrödinger equations and their solutions, *J. Aust. Math. Soc. Ser. B*, *25*, 16–43.

Plant, W. J., P. H. Dahl, J.-P. Giovanangeli, and H. Branger (2004), Bound and free surface waves in a large wind-wave tank, *J. Geophys. Res.*, *109*, C10002, doi:10.1029/2004JC002342.

Sedletskii, Y. V. (2003), The fourth-order nonlinear Schrödinger equation for the envelope of Stokes waves on the surface of a finite-depth fluid, *J. Exp. Theor. Phys.*, *97*, 180–193.

Shrira, V. I., and V. V. Geogjaev (2010), What makes the Peregrine soliton so special as a prototype of freak waves?, *J. Eng. Math.*, *67*, 11–22.

Slunyaev, A. V. (2005), A high-order nonlinear envelope equation for gravity waves in finite-depth water, *J. Exp. Theor. Phys.*, *101*(5), 926–941.

Ten, I., and H. Tomita (2006), Simulation of the ocean waves and appearance of freak waves, *Rep. RIAM Symp., 17SP1-2*, Kyushu Univ., Kasuga, Japan, 10–11 March.

Thrane, N., J. Wismer, H. Konstantin-Hansen, and S. Gade (2011), Practical use of the "Hilbert transform," Brüel and Kjær, Naerum, Denmark. [Available at http://www.bksv.com/doc/bo0437.pdf]

Zakharov, V. E. (1968), Stability of periodic waves of finite amplitude on a surface of deep fluid, *J. Appl. Mech. Tech. Phys.*, *2*, 190–194.

N. Akhmediev, Optical Sciences Group, Research School of Physics and Engineering, Australian National University, Canberra, ACT 0200, Australia.

A. Chabchoub, N. P. Hoffmann, and S. Neumann, Mechanics and Ocean Engineering, Hamburg University of Technology, D-21073 Hamburg, Germany. (amin.chabchoub@tuhh.de)